Mechanoreceptor distribution in stag beetle jaws corresponds to the material stress in fights

Reference:

Goyens Jana, Dirckx Joris, Aerts Peter.- Mechanoreceptor distribution in stag beetle jaws corresponds to the material stress in fights

Arthropod structure & development - ISSN 1467-8039 - 44:3(2015), p. 201-208

DOI: http://dx.doi.org/doi:10.1016/j.asd.2015.03.003

Handle: http://hdl.handle.net/10067/1261230151162165141

Goyens J, Dirckx J, Aerts P. (2015) ***Arthropod Structure and Development*** **44: 201-206**
Mechanoreceptor distribution in stag beetle jaws corresponds to the material stress in fights

Mechanoreceptor distribution in stag beetle jaws corresponds to the material stress in fights

J. Goyens[a,b]*, J. Dirckx[b] and P. Aerts[a,c]

[a]University of Antwerp, Laboratory of Functional Morphology, Universiteitsplein 1, B-2610 Antwerpen, Belgium
[b]University of Antwerp, Laboratory of Biophysics and BioMedical Physics, Groenenborgerlaan 171, B-2020 Antwerpen, Belgium
[c]Department of Movement and Sport Sciences, Ghent University, 9000 Ghent, Belgium
* Corresponding author: +3232652260, jana.goyens@uantwerpen.be

Male stag beetles (Lucanidae) use their extremely elongated jaws to pinch their rivals forcefully in male-male battles. The morphology of these jaws has to be a compromise between robustness (to withstand the bite forces), length and weight. *Cyclommatus metallifer* stag beetles circumvent this trade-off by reducing their bite force when biting with their slender jaw tips. Here we describe the functional mechanism behind the force modulation behaviour. Scanning Electron Microscopy and micro CT imaging show large numbers of small sensors in the jaw cuticle. We find a strong correlation between the distribution of these sensors and that of the material stress in the same jaw region during biting. The jaw sensors are mechanoreceptors with a small protrusion that barely protrudes above the undulating jaw surface. The sensors stimulate dendrites that extend from the neuronal cell body through the entire thickness of the jaw exoskeleton towards the sensors at the external surface. They form a sensory field that functions in a feedback mechanism to control the bite muscle force. This negative feedback mechanism enabled the stag beetles to evolve massive bite muscles without risking overloading their valuable jaws.

Keywords: sensory field, mechanical stress, animal weapon, *Cyclommatus metallifer,* Lucanidae, sexual selection

1. INTRODUCTION

Male stag beetles fight spectacular scuffles over mating rights with their sexually selected weaponry (Kawano, 2006; Tatsuta et al., 2001). In these battles, the males use their extremely large jaws as armature to grab, lift and throw their opponents (Goyens et al., 2015a; Shiokawa and Iwahashi, 2000). There is a large variation in mandible sizes within and between species (Gotoh et al., 2012, 2011; Kawano, 2006, 2000) and in some species, the jaws have evolved to be as long as their own body (Goyens et al., 2015a, 2015b; Kawano, 2006). Mandible size is determined by a combination of environmental (food availability) and genetic factors (Gotoh et al., 2012, 2011; Kawano, 2006, 2000), and the longer a male's jaws are, the higher its chance to win a battle (Gotoh et al., 2012; Goyens et al., 2015a). In some stag beetle species, this resulted in two male morph types: major males (with a large fighting apparatus but small wings) that fight over females and minor males (with large wings but rudimentary weaponry) that avoid fights (Kawano, 2006). However, in *Cyclommatus* stag beetles, one of the genera with the most oversized mandibles, the armature size variation is continuous and no male morph types can be distinguished.

The advantage of lengthy jaws in the wrestling phase of the fights, lies in its reach: long jaws are indispensable to haul and dislodge opponents (Goyens et al., 2015a, 2014b). But length was not the only selective pressure on the jaw morphology: the jaws also need to be as lightweight as possible, to

minimize the effect on the energy cost of running and flying. (Goyens et al., 2015b, 2015c). This explains the rather slender shape of the jaws. A third factor that shaped the jaw anatomy, is the enormous bite force developed during the battles. These bite forces are generated by massive closer muscles in the male head (Goyens et al., 2014a), representing a selective drive for strong, robust jaws. As a result, the existing jaw anatomy is almost certainly a compromise between reachability (long jaws), being lightweight (slender jaws) and withstanding high forces (robust jaws).

A combination of bite force measurements and Finite Element Analysis (FEA) revealed that stag beetles employ a behavioural (modulating) strategy to deal with this fragile balance: they reduce their muscle force when biting at the slender tips, to prevent breaking them (Goyens et al., 2014b). In this way they can keep the material stress at the slender tips at the same level as what is observed when biting at the robust teeth halfway along the mandibles (see e.g. arrows in Fig. 7A). This finding raises a new question: how do stag beetles control the muscle force modulation? We hypothesize that mechanoreceptors distributed in the jaw cuticle provide the essential feedback.

For many – probably all - animal species, information about their surroundings and their own body, is essential for various day-to-day tasks. For this purpose, insects have numerous types of sensors in their exoskeleton. These receptors are cuticular structures that transfer diverse stimuli: e.g. light, temperature, humidity, chemical or mechanical stimuli (Keil, 1997). Within the large and diverse family of mechanoreceptors, the cuticular components are adapted for a range of sensibilities: from very delicate air current receptors to robust sensors for contact (touch) and deformation (Keil, 1997; McIver, 1975).

The distribution of sensors has often proven to be related to the sensor's function. In rhinoceros beetles (*Trypoxylus dichotomus* (Linnaeus, 1771)), the anterior surface of the tips of their horns possesses the highest density of mechanoreceptors. This led to the conclusion that the horns do not only have a role as weapon, but also as a sensory structure to assess the size and position of opponents (McCullough and Zinna, 2013). The chemoreceptors of male *Agrotis exclamationis* (Linnaeus, 1758) moths that are specialized to detect the low-concentration female pheromones, are found on those parts of the antennae that experience the highest air currents (Hansson et al., 1986). Harvestmen (Opiliones) have a concentration of sensilla on the ventral parts of their legs, because these surfaces touch the substrate and food more readily than the lateral and dorsal regions. Moreover, the first leg pair is specialized to distinguish detailed features such as food, and hence contains more tactile sensors than the second leg pair (Willemart and Gnaspini, 2003).

We searched for sensors on *Cyclommatus metallifer* (Boisduval, 1835) stag beetle jaws and evaluated whether these could function in a feedback mechanism to modulate the bite force in order to avoid jaw failure. For this purpose, we used micro CT, Scanning Electron Microscopy (SEM) and Transmission Electron Microscopy (TEM) to investigate the sensor's micro structure and the correlation between their density and the material stress in the jaw while biting.

2. MATERIAL AND METHODS

2.1 Experimental animals

We obtained adult *C. metallifer* stag beetles from a commercial dealer (Kingdom of Beetle, Taiwan). We chose this stag beetle species due to its long jaws and eagerness to engage in fights (Goyens et al., 2015a, 2015b; Kawano, 2006).

2.2 Scanning Electron Microscopy

After sacrificing the animals, we visualised the external structures of the sensors with the Quanta 250 FEG microscope of the Electron Microscopy for Material Science group (EMAT) of the University of Antwerp. This microscope yields images with a spatial resolution up to 1 nm (FEI, Hillsboro, OR, USA). For this study, we used voltages of 10kV and 15kV. To view the internal structure of the sensors with SEM, we broke the mandibles transversely using the freeze fracturing technique and we checked the fracture surfaces for sensor structures that were still intact after the procedure.

2.3 Transmission Electron Microscopy

We performed TEM in search of a tubular body, which would indicate that the sensors are sensitive to mechanical stimuli. We cut a 1 mm x 0.3 mm piece from the distal medial side of the stag beetle mandible and fixed it in 2.5% buffered glutaraldehyde. The sample was post fixed for 2h at 4°C in 1% osmium tetroxide in veronal-acetate buffer and subsequently washed in the same buffer. After dehydration in steps of 50%, 70%, 90%, 95% and 100% ethanol, the sample was imbedded in EMBED 812 (Electron Microscopy Sciences, Hatfield, PA, USA). Next, we cut ultrathin sections with a Leica EM UC7 ultramicrotome (Leica Microsystems, Wetzlar, Germany). The sections were 60 µm thick, and were oriented (almost) parallel to the jaw surface. They were collected on Copper grids (Electron Microscopy Sciences, Hatfield, PA, USA), stained with 2% uranyl acetate and buffered Reynolds solution, and examined with a Tecnai Spirit (FEI, Hillsboro, OR, USA).

2.4 Micro CT imaging of the tip of a male jaw

Micro CT imaging was used to scan the internal structure of the jaw tip. We scanned the stag beetle jaws with a Skyscan 1172 high resolution micro CT scanner (Bruker microCT, Kontich, Belgium; see Table 1). The jaws were stained with iodine in an ethanol solution, which provides a very good visualisation of soft tissues (Goyens et al., 2014a). We carefully positioned the very tip of one of the mandibles (2.55 mm long) on the object stage of the micro CT scanner. By manually optimizing the scan parameters (see Table 1), we could obtain a resolution of 0.96 µm, which is close to the highest detectability that can be achieved by the scanner according to the manufacturer (0.7 µm; Bruker microCT, Kontich, Belgium).

Table 1: Micro CT scan parameters

	Jaw tip	**Entire jaw 1**	**Entire jaw 2 & 3**
Filter	No	No	No
Voltage	36 kV	70 kV	44 kV
Current	222 µA	141 µA	222 µA
Rotation angle	0.3°	0.2°	0.2°
Frame averaging	6	5	5
Exposure time	1650 ms	440ms	490ms
Pixel size	0.96 µm	4.1 µm	3.96 µm
Reconstructed slice images	2656	9466	10354
Scan duration	143 min	77 min	410 min

2.5 Micro CT imaging of the entire male jaws

We determined the sensor distribution with micro CT scans of the entire jaw of three male individuals (Skyscan 1172 high resolution micro CT scanner; see Table 1). The external cuticular portion of the sensors was barely discernible on the micro CT scans, but dendrite channels through the entire thickness of the jaw exoskeleton were clearly visible as fluctuations of the grey values inside the mandible (which highlight material differences). Since each sensor on the outer surface of the mandible has such a channel, their distribution is identical. In order to visualise the distribution of the channels, we selected the darker voxels with the 3D image processing software Amira (Amira 5.4.4; 64-bit version, FEI, Hillsboro, OR, USA). For this laborious task, we used a combination of automatic thresholds, based on grey scale values, with manual corrections in the three orthogonal views.

We manually counted the sensors in 28 square patches of 1 mm^2 on the three jaws (see Fig. 1), which enabled a quantified comparison between the number of sensors and the material stress that is predicted by Finite Element modelling (Goyens et al., 2014b). These patches were equally spaced on the dorsal and ventral jaw surfaces and the inner and outer lateral surfaces (see Fig. 1).

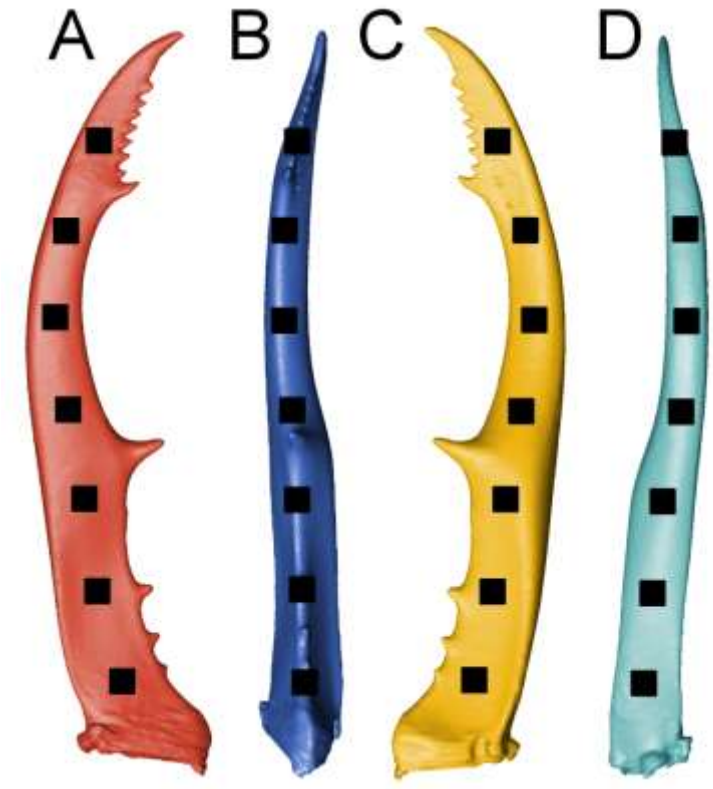

Figure 1: Location of the square 1 mm^2 patches that were used to count the number of sensors in the dorsal (A), medial (B), ventral (C) and lateral (D) jaw surface.

3. RESULTS

3.1 Scanning Electron Microscopy

The sensors are easily recognisable on the SEM images. They appear as little dots on low resolution images (see Fig. 2A,B). Considerable wear (resulting from the natural jaw use) is visible on the tips: because of the relative position of both mandibles, the tips scuff against each other. Images with a higher resolution show that the sensors are broken off in these damaged zones (see Fig. 3). Apart from in the tip region, however, most of the sensors are intact. They possess small protrusions (ca 15 µm long) that barely extend above the undulating exoskeleton surface (see Fig. 2C,D). Sometimes, these protrusions are peg-shaped instead of straight. We did not find pores on the protrusions, which indicates that they have no chemosensory function. The sensor protrusions have a smooth surface and are placed within a round (or occasionally slightly elliptical) pit, which is the typical structure of mechanosensors in insects (Keil, 1997; McIver, 1975). They have a different anatomy than the mechanosensors that detect contact at the very base of the mandibles and at the tibia (see Fig. 4): the sensory hairs of these contact receptors are more than 5 times longer than the protrusions described above, they often have a scaled surface and sometimes they split at the distal end.

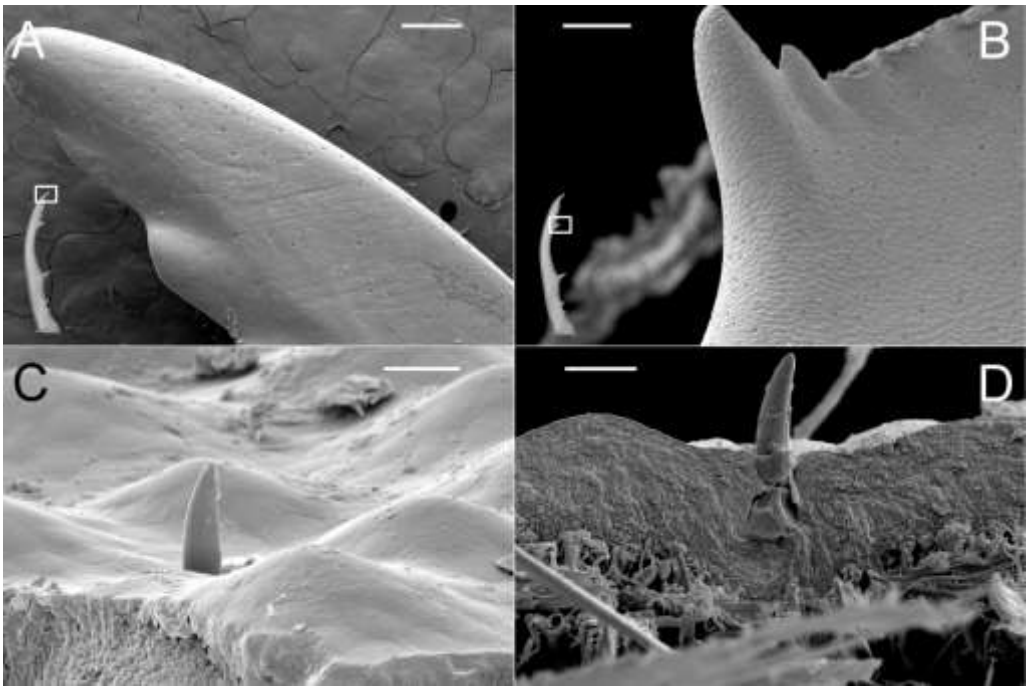

Figure 2: SEM of the stag beetle jaw. Top panels: larger view on the tip of the jaw, the location of the picture on the jaw is indicated on the inset. A lot of sensors are visible as small dots. The scale bars indicate 250 µm. Bottom panels: detailed view on two sensors. The scale bars indicate 10 µm. The right bottom panel (D) shows a sensor on a fracture surface through the cuticle, which gives an insight on the structures below the surface. Chitin fibres of the lower layer of cutide are visible.

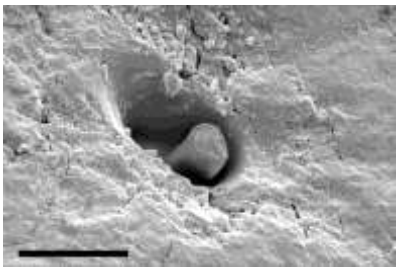

Figure 3: oblique SEM view on a broken sensor. The cuticula surface around the sensor shows heavy wear. The scale bar indicates 10 µm.

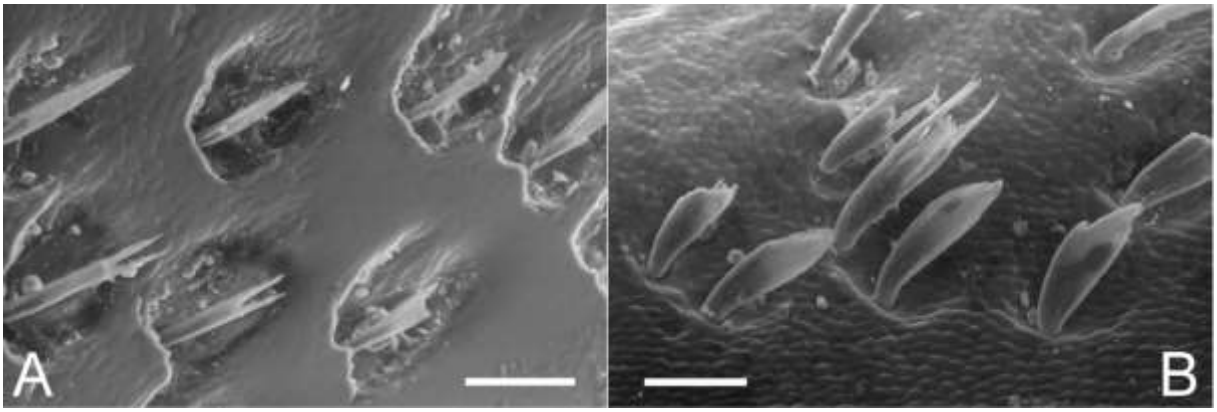

Figure 4: SEM of contact sensors on the mandible base (A) and tibia of the fore limb (B). The scale bars indicate 50 µm.

3.2 Micro CT imaging of the tip of a male jaw

The micro CT scan at maximum resolution provides a detailed view on the internal structures of the sensors (0.96 µm voxel size; see Fig.5). At the inner aperture of the channels, we can see flattened cells (see *a* in figure 5) that send long and thin extensions through the channels (see *b* in figure 5) towards the cuticular part of the sensor at the outer aperture of the channel. Similar extensions reach along the inside surface of the cuticle (see *c* in Fig. 5) towards neighbouring cells. The observed structures are thus interpreted as the neural field of the sensors.

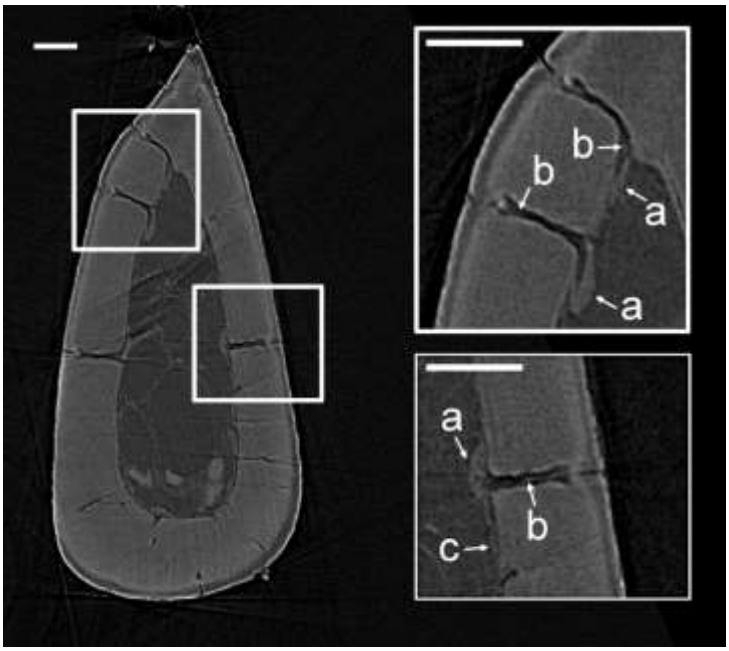

Figure 5: Cross-section through the tip of a male jaw. Several channels through the jaw cuticle are visible. Three channels are enlarged in the insets, and neuron cell bodies at the inner end of the channel are visible (a), as well as their extensions towards the sensors (b) and to other neurons (c). The scale bars indicate 100 µm.

3.3 Transmission electron microscopy

TEM provides a more detailed view on the internal dendrite structures. On TEM sections through the distal tip of the sensory dendrite, we see a high number of densely packed microtubules in an electron-dense material: a tubular body with an almost circular cross-section (see Fig. 6).

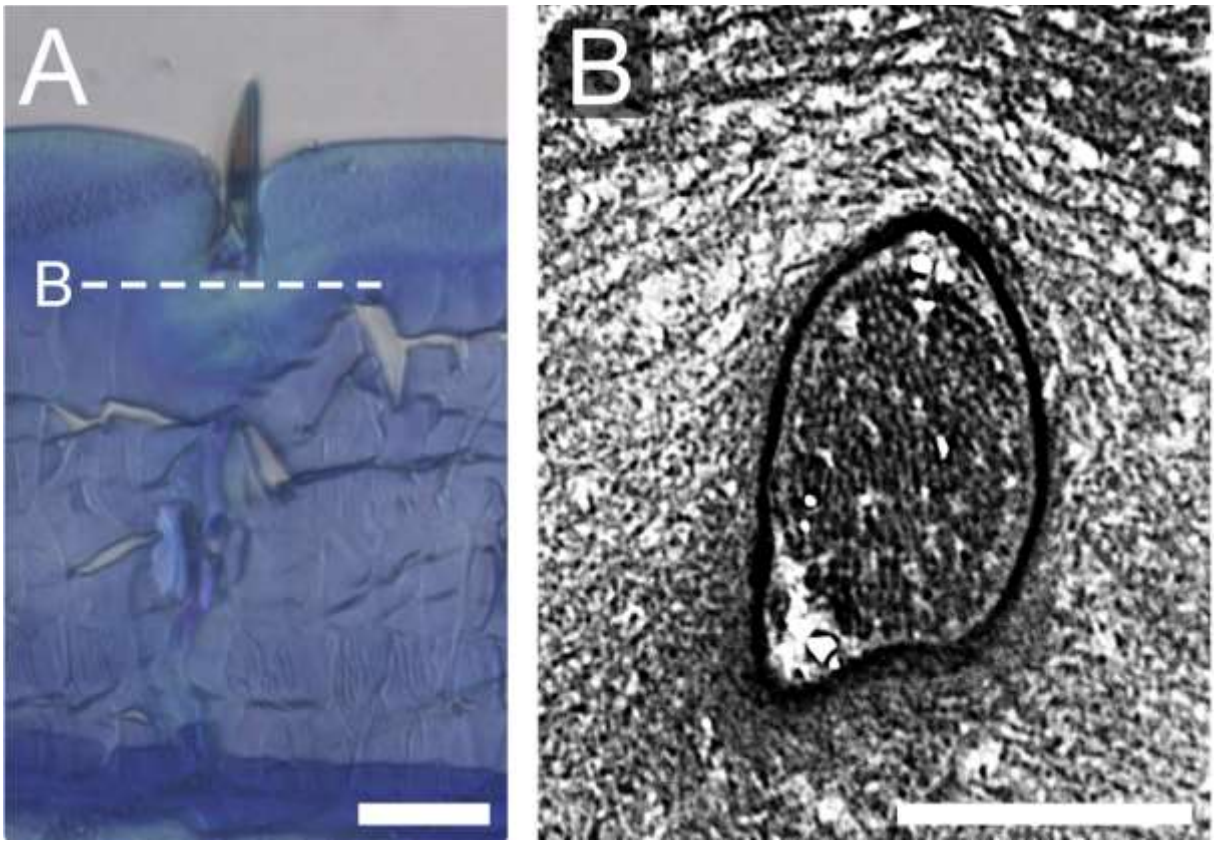

Figure 6: A: Light microscopic image, normal to the jaw surface, showing the approximate location (dashed line) of B. The scale bar indicates 20 µm. B: almost transverse (slightly oblique) section through the dendrite tip, showing the tubular body. The scale bars indicate 1 µm.

3.4 Micro CT imaging of the entire male jaws

Figure 7 shows two cross-sections through the male jaws, as obtained by micro CT imaging with 4.1 µm voxels size. The channels through the cuticle of the mandible are still visible on these images. In Figure 8, the distribution of these channels (i.e. of the sensors) is depicted. We observe a very distinct pattern: there are sensors present in the entire jaw, but the concentration varies greatly. The concentration rises from the base of the mandible to the tips. At the proximal half of the mandibles, the jaws have a triangular cross-section (see Figure 7C). The three vertices of this triangular cross-section form 'ridges' (ribs) in the external surface of the exoskeleton (see e.g. Fig 8). We observe a high sensors density in these three ridges.

When we compare the location of the sensors (see Fig. 8) with the material stress that is calculated by FEA (see Fig. 9), we see a strong correlation between both: the sensor density as well as the material stress is elevated at the tip and at the ridges (especially the inner ridge). This visual correspondence is confirmed in figure 10: we see a strong correlation between the number of sensors and the material stress at the same location. The overall correlation is statistically significant (Pearson's correlation coefficient DF= 82; ρ=0.84; $p<0.001$). The slope of this correlation is significantly different between the sides of the jaw: the medial surface has the lowest slope (see Fig. 10; ANCOVA: p_{group}=0.73, $p_{slope}<0.001$, $p_{interaction}<0.001$).

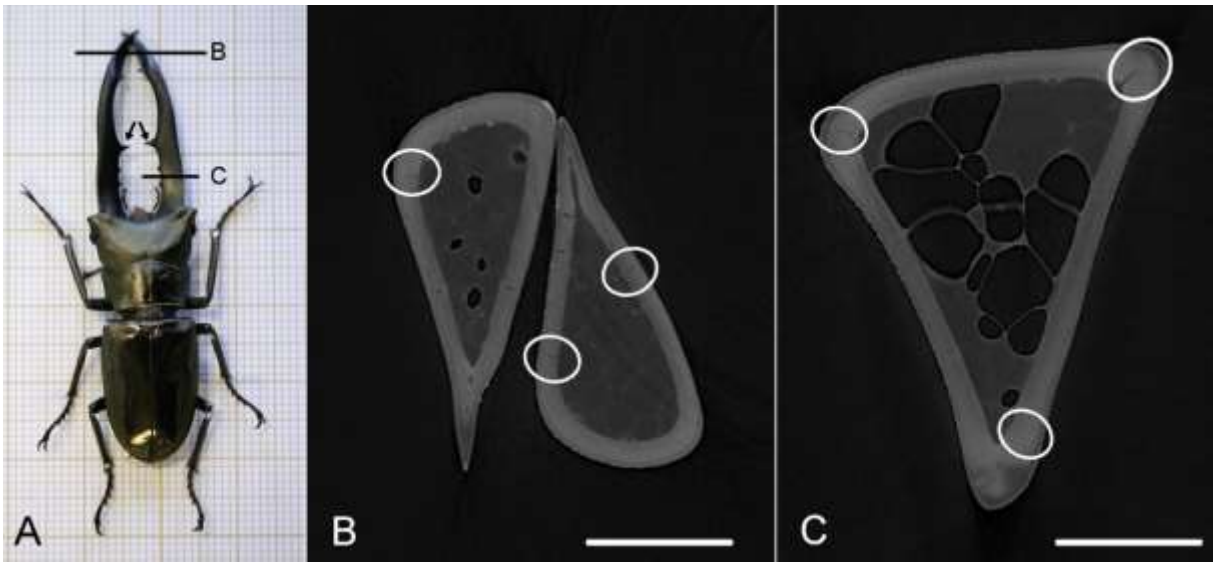

Figure 7: A: Photo of a male *Cyclommatus metallifer* stag beetle. The robust teeth halfway the mandibles are indicated with arrows. B and C: Micro CT image with voxel size 4.1 µm. Several little channels through the exoskeleton are visible, of which 6 are encircled. The location of the sections in B and C are indicated with black lines in A. The scale bars indicate 1 mm.

Figure 8: Distribution of the sensors in the male jaw. The jaw cuticle is depicted in transparent orange and the dendrite channels are shown in purple. In lateral view (e.g. in the ribs of the jaw), these channels appear as dashes, while in top view they look like dots. A: Jaw in dorsal (top) view. B: Lateral view (outside). C: Medial view (inside). The scale bar indicates 1 cm.

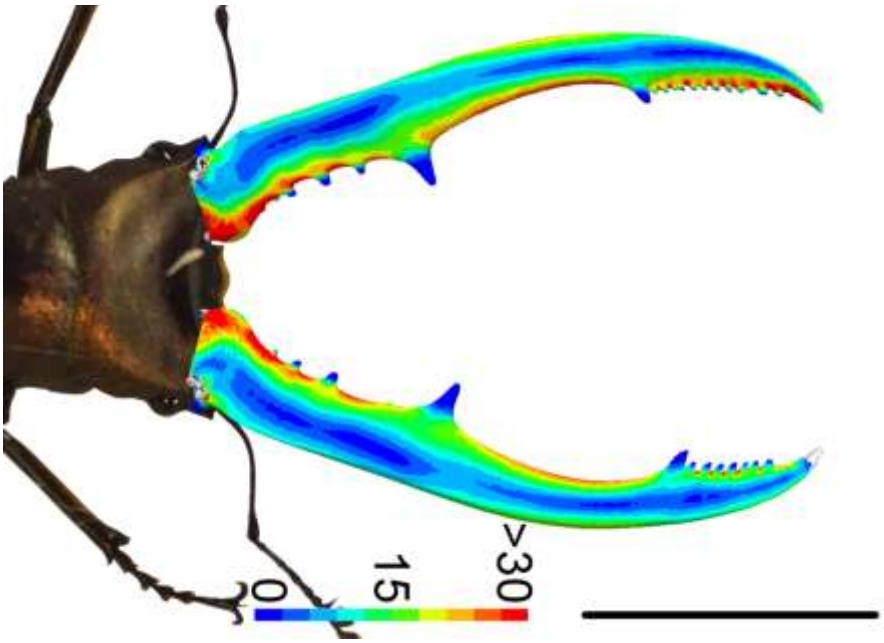

Figure 9: Picture of a male stag beetle and Finite Element models showing the Von Mises stress (MPa) distribution in both jaws during tip biting. The right jaw was used in the comparison with the sensor distribution. The scale bar indicates 1 cm. Adapted from (Goyens et al., 2014b).

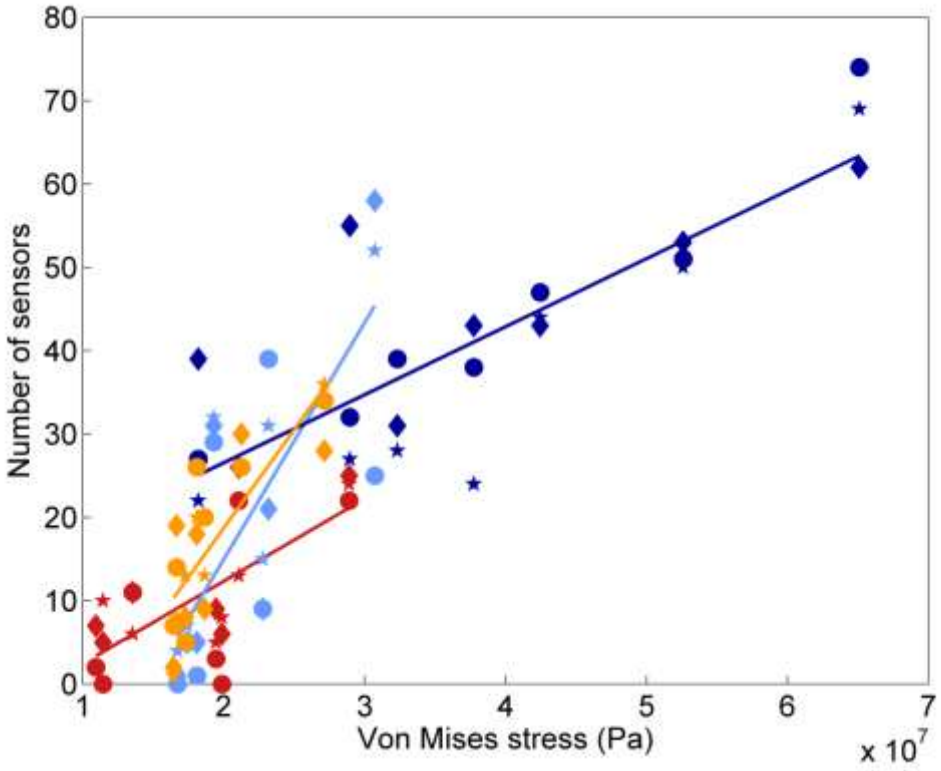

Figure 10: Correlation between material stress (Von Mises stress) and the number of sensors for 28 patches on the dorsal (red), ventral (orange), lateral (light blue) and medial (dark blue) sides of the jaw. The three individuals are indicated with different symbols.

4. DISCUSSION

The observation that male stag beetles modulate their bite force to avoid breaking their jaws, led to the present search for sensors (Goyens et al., 2014b). SEM and micro CT reveal that the mandibles indeed contain a high number of sensors. TEM further shows that the dendrite tip of the sensors contains a tubular body, which proofs that they sense mechanical stimuli (Keil, 2012). Finally, we find that the sensors are distributed according to the distribution of the material stress that is imposed by biting. Together, these observations strongly suggest that we have found a system of mechanosensors that functions in a negative feedback system to regulate bite force in order to prevent jaw failure.

The sensors on the stag beetle jaws have a small protrusion (ca 15 µm long). Hence, they are not campaniform sensilla, the typical strain sensor in insects, which have a dome-shaped cupola instead of a hair (Keil, 1997). Rather, the sensor morphology resembles that of the bristle type of mechanoreceptors, albeit with a very short hair that barely elevates above the undulating jaw surface. Their morphology is also different from that of other bristle-type sensors on the stag beetle body (compare Figs. 2 and 4). Bristle mechanoreceptors are constructed as first order levers, and stimulate the dendrite tip when the bristle is deflected (Keil, 1997). The methods in the current paper do not allow us to determine how exactly the mechanical deformations (strains) of the jaw exoskeleton are transmitted into neuronal signals. We hypothesise that jaw bending causes small deflections of the tiny bristle-shaped sensors that are suspended in the exoskeleton. As is common in bristle mechanosensors, these sensor deflections would subsequently be transmitted to the dendrite tip. This functional mechanism seems plausible because stag beetles bite extremely forcefully, which causes macroscopic jaw deformations (Goyens et al., 2014a, 2014b).

The tubular body and the sensor socket have nearly circular cross-sections. Therefore, the sensitivity of the sensors is probably not direction-dependent. The sensitivity does however depend on the sensor density, as a higher number of receptors probably leads to a more precise measurement. The same was found for the sensor sensitivity of resource recognition in harvestmen (Willemart and Gnaspini, 2003). This explains the functional advantage of the high sensor concentrations in the stag beetle jaws at those locations where FEA predicts high material stress. Also in other arthropod taxa, there is a strong correlation between the location and function of sensors (Hansson et al., 1986; McCullough and Zinna, 2013; Willemart and Gnaspini, 2003). In case of the stag beetle jaws, the high number of sensors in the ridges can probably also be attributed to the stress concentration at sharp edges of ridges (Pilkey and Pilkey, 2008), and further, the high number of sensors at the jaw tip may also be necessary because they often get damaged when the mandibles scuff against each other.

It can be questioned whether or not the large concentrations of 'sensor' -channels in the exoskeleton weaken the strength or integrity of the mandibular structure (i.e. comparable with concentrations of micro-cracks). This is probably not the case. First, the channels are not large enough to pose a fracture risk (Vincent et al., 2007). Second, the channels in the exoskeleton were created during the formation of the cuticle. Hence, the fibres lie around the holes, rather than being interrupted by them as in the case of micro cracks. This makes the cuticle less prone to fracture (Skordos et al., 2002; Vincent et al., 2007). Therefore, the sensory field enables a feedback system to prevent failure, without weakening the structure any further.

5. CONCLUSION

We detected a field of mechanoreceptive sensilla in the mandibles of male *C. metallifer* stag beetles. The distribution of the sensors in this field corresponds strongly to the material stress that the jaws experience during biting. Therefore, the stag beetles can probably control and modulate their bite force during fights using these sensors in a feedback mechanism. This finding may shed light on the evolution of the stag beetle mandible morphology. The armature evolution faced a complex interaction of trade-offs between mandible weight, size and robustness. A sensory feedback system enables the stag beetles to partially and temporarily evade these interactions, which may have paved the way for the evolution of their impressive weaponry and its massive bite muscles.

ACKNOWLEDGEMENTS

The authors thank Ms. Carine Moers, Dr. Isabel Pintelon and Prof. Jean-Pierre Timmermans of the Laboratory of Cell Biology & Histology at the University of Antwerp for the TEM; and Mr. Nicolaas Lousberg, Mr. Stijn Van den broeck and Prof. Sara Bals of the Electron Microscopy for Material Science group at the University of Antwerp for the SEM.

The present study was funded by a BOF grand (ID BOF UA 2011-445-a) of the Research Council of University of Antwerp. The SkyScan 1172 high resolution micro CT scanner, located at the VUB facilities, was funded by the Hercules Foundation of the Flemish Government (grant UABR/11/004). The Quanta 250 FEG microscope of the Electron Microscopy for Material Science group at the University of Antwerp was partly funded by the Hercules foundation of the Flemish Government. The Tecnai G2 Spirit BioTWIN TEM and Leica Ultracut EM UC7 ultramicrotome of the Laboratory of Cell Biology & Histology at the University of Antwerp were purchased with support of the Hercules Foundation of the Flemish Government (grants AUHA004 and AUHA11/01).

REFERENCES

Gotoh, H., Cornette, R., Koshikawa, S., Okada, Y., Lavine, L.C., Emlen, D.J., Miura, T., 2011. Juvenile Hormone Regulates Extreme Mandible Growth in Male Stag Beetles. PLoS One 6, e211139. doi:10.1371/journal.pone.0021139

Gotoh, H., Fukaya, K., Miura, T., 2012. Heritability of male mandible length in the stag beetle Cyclommatus metallifer. Entomol. Sci. 15, 430–433. doi:10.1111/j.1479-8298.2012.00527.x

Goyens, J., Dirckx, J., Aerts, P., 2015a. Stag beetle battle behaviour and its associated anatomical adaptations (In Press). J. Insect Behav.

Goyens, J., Dirckx, J., Aerts, P., 2015b. Costly sexual dimorphism in Cyclommatus metallifer stag beetles. Funct. Ecol. 29, 35–43. doi:10.1111/1365-2435.12294

Goyens, J., Dirckx, J., Dierick, M., Van Hoorebeke, L., Aerts, P., 2014a. Biomechanical determinants of bite force dimorphism in *Cyclommatus metallifer* stag beetles. J. Exp. Biol. 217, 1065–1071. doi:10.1242/jeb.091744

Goyens, J., Soons, J., Aerts, P., Dirckx, J., 2014b. Finite Element modelling reveals force modulation of jaw adductors in stag beetles. J. R. Soc. Interface 11, 20140908. doi:10.1098/rsif.2014.0908

Goyens, J., Van Wassenbergh, S., Dirckx, J., Aerts, P., 2015c. Cost of Flight and the Evolution of Stag Beetle Weaponry (In Press). J. R. Soc. Interface.

Hansson, B.S., Löfstedt, C., Löfqvist, J., 1986. Spatial arrangement of different types of pheromone-sensitive sensilla in a male moth. Naturwissenschaften 73, 269–270.

Kawano, K., 2000. Genera and allometry in the stag beetle family Lucanidae, Coleoptera. Ann. Entomol. Soc. Am. 93, 198–207. doi:10.1603/0013-8746(2000)093

Kawano, K., 2006. Sexual dimorphism and the making of oversized male characters in beetles (Coleoptera). Ann. Biomed. Eng. 99, 327–341. doi:10.1603/0013-8746(2006)099

Keil, T., 1997. Functional morphology of insect mechanoreceptors. Microsc. Res. Tech. 39, 506–31. doi:10.1002/(SICI)1097-0029(19971215)39:6<506::AID-JEMT5>3.0.CO;2-B

Keil, T.A., 2012. Sensory cilia in arthropods. Arthropod Struct. Dev. 41, 515–34. doi:10.1016/j.asd.2012.07.001

McCullough, E.L., Zinna, R.A., 2013. Sensilla Density Corresponds to the Regions of the Horn Most Frequently Used During Combat in the Giant Rhinoceros Beetle Trypoxylus dichotomus (Coleoptera: Scarabaeidae: Dynastinae). Ann. Entomol. Soc. Am. 106, 518–523.

McIver, S.B., 1975. Structure of cuticular mechanoreceptors of arthropods. Annu. Rev. Entomol. 20, 318–397. doi:10.1146/annurev.en.20.010175.002121

Pilkey, W., Pilkey, D., 2008. Peterson's Stress Concentration Factors, 3rd Edition. John Wiley and Sons, Hoboken, New Jersey.

Shiokawa, T., Iwahashi, O., 2000. Mandible dimorphism in males of a stag beetle, Prosopocoilus dissimilis okinawanus (Coleoptera: Lucanidae). Appl. Entomol. Zool. 35, 87–494. doi:10.1303/aez.2000.487

Skordos, a, Chan, P.H., Vincent, J.F. V, Jeronimidis, G., 2002. A novel strain sensor based on the campaniform sensillum of insects. Philos. Trans. A 360, 239–53. doi:10.1098/rsta.2001.0929

Tatsuta, H., Mizota, K., Akimoto, S., 2001. Allometric patterns of Heads and Genitalia in the stag beetle Lucanus maculifemoratus (Coleoptera: Lucanidae). Ann. Entomol. Soc. Am. 94, 462–466. doi:10.1603/0013-8746(2001)094[0462:APOHAG]2.0.CO;2

Vincent, J.F. V, Clift, S.E., Menon, C., 2007. Biomimetics of Campaniform Sensilla: Measuring Strain from the Deformation of Holes. J. Bionic Eng. 4, 63–76.

Willemart, R.H., Gnaspini, P., 2003. Comparative Density of Hair Sensilla on the Legs of Cavernicolous and Epigean Harvestmen (Arachnida: Opiliones). Zool. Anz. 242, 353–365.